Earth conduction effects in systems of overhead and underground conductors in multilayered soils

D.A. Tsiamitros, G.C. Christoforidis, G.K. Papagiannis, D.P. Labridis and P.S. Dokopoulos

Abstract: Electromagnetic interference calculations in the case of overhead lines and underground insulated conductors require the determination of the self and mutual impedances of all conductors in the arrangement. For the calculation of these impedances in nonhomogeneous soils, the use of the finite-element method is suggested. However, this is generally a complicated and time-consuming task. Analytic expressions for these impedances are derived by a solution of the electromagnetic field equations for the case of *n*-layer soil. The infinite integrals involved are evaluated using a numerically stable and efficient integration scheme. A typical transmission line/underground insulated pipeline arrangement is examined for various two-layer earth models and over a wide frequency range. The validity of the proposed methodology is justified by a proper finite-element method formulation. The inclusion of earth stratification leads to substantially different results for the calculated impedances. These differences affect significantly the levels of voltages and currents induced on the pipeline, even for power frequencies, justifying the need for a more detailed earth model representation.

1 Introduction

A research topic that has received significant attention from researchers during recent decades is the electromagnetic interference between overhead power transmission lines and electric traction lines or underground insulated conductors. The result of this interference is the induction of voltages and currents on the underground insulated conductors, which may cause electric shocks, deterioration of coating, damage of equipment connected to the underground insulated conductor and corrosion. The various approaches used to calculate the levels of the induced voltages and currents are described in [1–5]. All these approaches are based on the solution of equivalent circuits describing the system of the transmission line and the underground conductor and require the calculation of the per-unit-length self and mutual impedances between all conductors of the arrangement.

The impedances of the system are strongly influenced by the presence of the lossy earth. For the case of overhead lines, the earth return impedances are calculated using the widely accepted Carson's formulas [6]. Pollaczek [7] has proposed similar formulas applicable to cases of underground conductors and to combinations of underground and overhead conductors. In both approaches the earth is assumed to be homogeneous and semi-infinite. These expressions contain complex, highly oscillatory, semi-infinite integrals, which are difficult to evaluate numerically. Several approaches have been proposed for the practical calculation of the earth correction terms, either in the form of approximate formulas [8], or in the form of algorithmic approximations [9].

A further complication is due to the fact that the earth is composed of several layers of different electromagnetic properties. Solutions for overhead conductors above multi-layer earth have been proposed early enough [10, 11], but these solutions do not apply to the case of underground insulated conductors. The research in this area did not proceed, possibly due to the lack of accurate data for proper earth modelling. In some recent publications however [12–15], several numerical techniques are proposed, offering reliable estimations of the multilayered earth parameters, based on actual earth surface resistivity measurements.

A very efficient approach in nonhomogeneous earth treatment is the use of the finite-element method (FEM) for the calculation of the impedances of various conductor arrangements. The FEM is a numerical method used for the solution of electromagnetic field equations in a region, regardless of its geometric complexity. In a recent extension [16] the FEM is applied for the calculation of the impedances of transmission lines over nonhomogeneous earth structures. A similar methodology is used in [17, 18] for the calculation of the impedances between overhead transmission lines and underground insulated metal pipelines, as the first step of a hybrid method for the calculation of the induced voltages and currents on pipelines. A major drawback is the complexity in the application of the FEM, which is usually a time-consuming task, requiring access to proper software.

The scope of this paper is to present analytic expressions for the calculation of the per-unit-length self and mutual earth return impedances of an overhead–underground conductor system for the generalised case of a *n*-layer earth. These expressions are derived by a general solution of the electromagnetic field equations, using a methodology based on the hertzian vector approach. This methodology, initially presented in [19] for underground cables in a two-layer earth, is extended for the combination of overhead and underground conductors and is generalised for a *n*-layer earth case.

IEE Proceedings online no. 20050195

doi:10.1049/ip-gtd:20050195

Paper first received 24th May and in final revised form 8th December 2005

The authors are with Power Systems Laboratory, Dept. of Electrical & Computer Engineering, Aristotle University of Thessaloniki, P.O. Box 486, GR-54124 Thessaloniki, Greece

E-mail: grigoris@eng.auth.gr

The resulting expressions are similar in form to the corresponding proposed by Pollaczek [7] and Sunde [10], containing complex semi-infinite integral terms. These terms are evaluated using a new numerical integration scheme [20]. This scheme is based on proper combinations of numerical integration methods, to overcome efficiently the problems due to the highly oscillatory form of the infinite integrals. The scheme has been applied in several cases of cable impedance calculations in both homogeneous and multilayered earth structures [19, 20] and proved to be numerically stable and efficient in all examined cases.

The accuracy of the results obtained by the new methodology is checked using a proper FEM formulation in a test system, consisting of a typical single-circuit overhead transmission line and an insulated pipeline buried in different two-layer earth structures. The earth parameters for each structure have been estimated from actual ground resistivity measurements [12]. The comparison with the results obtained by the FEM verifies the validity of the proposed expressions and the accuracy of the numerical integration scheme.

The impedances calculated for the two-layer earth model differ greatly from those calculated considering a homogeneous earth. These differences lead to significant divergence in the level of the induced voltages and currents on the pipeline, showing that a more accurate model than the simple homogeneous earth model should be used in the electromagnetic interference calculations.

2 Problem formulation and solution

2.1 Electromagnetic field equations

The general layout of a system consisting of an overhead and an underground insulated conductor in a n-layer earth structure is shown in Fig. 1. The underground insulated conductor is buried in the mth layer of the n-layer earth. The vertical distance of the underground insulated conductor from the upper boundary of the layer is h_1. The vertical distance of the overhead conductor from the earth surface is h_2. The horizontal separation distance between the two conductors is y_{ik}. The ith layer has permeability μ_i, permittivity ε_i and conductivity σ_i. The air has a conductivity σ_0 equal to zero, permeability μ_0 and permittivity ε_0 equal to those of the free space. The nth layer is considered to be of infinite depth.

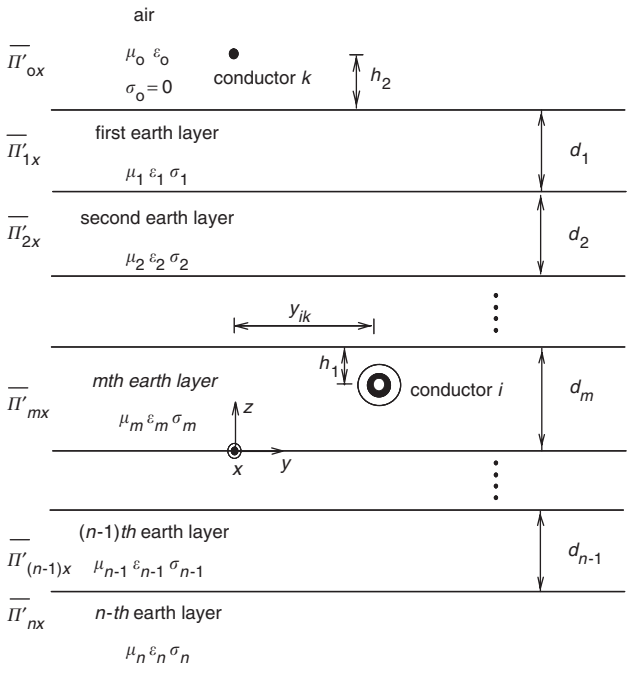

Fig. 1 *Geometric configuration of system comprising of overhead and underground insulated conductor in n-layered earth*

The mutual impedances between the two conductors may be derived by integrating the field due to the conductor dipoles. The field intensities and potentials can be expressed in terms of a single vector function $\overline{\Pi}$, usually referred to as the hertzian vector [10]. The $\overline{\Pi}$ function has been adopted for the solution of the electromagnetic field equations in this paper. Assuming a quasi-TEM propagation mode, following assumptions apply.

First a filamentary current source of infinite length is assumed to be located at the conductor centre. In the case of self impedances, the unequal current density on the conductor surface due to the skin effect is taken into account by means of proper internal impedance terms. These terms are calculated by the well-known skin effect formulas [21, 22] using modified Bessel functions [23] and can be added to the self-impedance terms.

The second assumption is that the thickness of the insulation of the underground insulated conductor is negligible compared to its diameter. The impedance of the insulation can be calculated using a simple formula [21] and can be also added to the corresponding impedances.

Finally the conductors are assumed to be uniform and of infinite length, thus the end effects can be neglected and therefore only the x-components of the hertzian vector $\overline{\Pi}$ are used in the analysis.

Assuming a horizontal dipole with a moment Ids in the place of the overhead conductor in Fig. 1, the x-components of the $\overline{\Pi}$ function in the air and in the several earth layers are defined as $\overline{\Pi}'_{0x}, \overline{\Pi}'_{1x}, \overline{\Pi}'_{2x}, \ldots, \overline{\Pi}'_{mx}, \ldots, \overline{\Pi}'_{nx}$. The equation that describes $\overline{\Pi}'_{0x}$ at any point in the air with co-ordinates (x, y, z) is [11]

$$\overline{\Pi}'_{0x} = \int_0^\infty \left[\overline{C} \frac{u}{\overline{\alpha}_0} e^{-\overline{\alpha}_0 |z-(d_1+d_2+\cdots+d_m+h_2)|} + \overline{g}'_0(u) e^{-\overline{\alpha}_0 z} \right] \times J_0(ru)du, \quad z \geq d_1 + d_2 + \cdots + d_m \tag{1}$$

and

$$\overline{\Pi}'_{1x} = \int_0^\infty \left[\overline{f}'_1(u) e^{\overline{\alpha}_1 z} + \overline{g}'_1(u) e^{-\overline{\alpha}_1 z} \right] J_0(ru)du, \quad d_2 + \cdots + d_m \leq z \leq d_1 + d_2 + \cdots + d_m \tag{2}$$

$$\overline{\Pi}'_{mx} = \int_0^\infty \left[\overline{f}'_m(u) e^{\overline{\alpha}_m z} + \overline{g}'_m(u) e^{-\overline{\alpha}_m z} \right] J_0(ru)du, \quad 0 \leq z \leq d_m \tag{3}$$

and

$$\overline{\Pi}'_{nx} = \int_0^\infty \overline{f}'_n(u) e^{\overline{\alpha}_n z} J_0(ru)du, \quad z \leq -(d_{m+1} + \cdots + d_{n-1}) \tag{4}$$

where $\overline{C} = j\omega\mu_0 Ids/4\pi\overline{\gamma}_0^2$. In these relations, $J_0()$ is the Bessel function of the first kind of zero order, $r = \sqrt{x^2 + y^2}$, $\overline{\alpha}_i = \sqrt{u^2 + \overline{\gamma}_i^2}$, $\overline{\gamma}_i^2 = j\omega\mu_i(\sigma_i + j\omega\varepsilon_i)$, where $i = 0, 1, 2, \ldots, n$, j is the imaginary unit and $\omega = 2\pi f$ is the angular velocity. Equations (1)–(4) are used in [11] to derive the per-unit-length impedance expressions of the overhead conductors only. Thus the aim in this paper is to derive the mutual impedance expression between the

overhead and the underground insulated conductor and the self impedance of the underground insulated conductor.

2.2 Determination of per-unit-length mutual impedance

The boundary conditions are [11]

$$\overline{\gamma}_{k-1}^2 \overline{\Pi}'_{(k-1)x} = \overline{\gamma}_k^2 \overline{\Pi}'_{kx} \tag{5}$$

$$\frac{1}{\mu_{k-1}} \overline{\gamma}_{k-1}^2 \frac{\partial \overline{\Pi}'_{(k-1)x}}{\partial z} = \frac{1}{\mu_k} \overline{\gamma}_k^2 \frac{\partial \overline{\Pi}'_{kx}}{\partial z} \tag{6}$$

where $k = 1, 2, \ldots, n$. Substituting (1) and (2) in (5) and (6), (7) and (8) are produced. Substituting the remaining $\overline{\Pi}$ functions in (5) and (6), $2n-2$ similar equations are derived

$$\overline{\gamma}_0^2 \left(\overline{C} \frac{u}{\overline{\alpha}_0} e^{-\overline{\alpha}_0 h_2} + \overline{g}'_o e^{-\overline{\alpha}_0 (d_1 + d_2 + \cdots + d_m)} \right) = \overline{\gamma}_1^2 \left(\overline{f}'_1 e^{\overline{\alpha}_1 (d_1 + d_2 + \cdots + d_m)} + \overline{g}'_1 e^{-\overline{\alpha}_1 (d_1 + d_2 + \cdots + d_m)} \right) \tag{7}$$

$$\frac{\overline{\alpha}_0}{\mu_0} \overline{\gamma}_0^2 \left(\overline{C} \frac{u}{\overline{\alpha}_0} e^{-\overline{\alpha}_0 h_2} - \overline{g}'_o e^{-\overline{\alpha}_0 (d_1 + d_2 + \cdots + d_m)} \right) = \frac{\overline{\alpha}_1}{\mu_1} \overline{\gamma}_1^2 \left(\overline{f}'_1 e^{\overline{\alpha}_1 (d_1 + d_2 + \cdots + d_m)} - \overline{g}'_1 e^{-\overline{\alpha}_1 (d_1 + d_2 + \cdots + d_m)} \right) \tag{8}$$

Solving the system of the $2n$ equations, $\overline{f}'_m$ and $\overline{g}'_m$ are obtained. The general form of the $2n-2$ equations and the exact form of the $\overline{f}'_m$ and $\overline{g}'_m$ functions are shown in the Appendix (Section 8.1). Thus the $\overline{\Pi}$ function in the mth layer $\overline{\Pi}'_{mx}$ is completely defined. The per-unit-length mutual impedance between the overhead conductor k and the underground insulated conductor i can then be derived by integrating $\overline{\Pi}'_{mx}$ along the infinite conductor k, i.e. along the x-axis [10]

$$\overline{Z}'_{ik} = \int_{-\infty}^{\infty} \left[\overline{\gamma}_m^2 \frac{\overline{\Pi}'_{mx(z=d_m - h_1, y=y_{ik})}}{IdS} \right] dx \tag{9}$$

By replacing $\overline{\Pi}'_{mx}$ from (3), $\overline{Z}'_{ik}$ takes the form of (10a). The term $\int_{-\infty}^{\infty} J_0(u\sqrt{x^2 + y_{ik}^2})dx$ can be substituted by $2\cos(uy_{ik})/u$, as in [23], resulting in (10b)

$$\overline{Z}'_{ik} = \overline{\gamma}_m^2 \int_0^{\infty} \frac{\left[\overline{f}'_m(u) e^{\overline{\alpha}_m (d_m - h_1)} + \overline{g}'_m(u) e^{-\overline{\alpha}_m (d_m - h_1)} \right]}{IdS} \times \left[\int_{-\infty}^{\infty} J_0(u\sqrt{x^2 + y_{ik}^2})dx \right] du \tag{10a}$$

$$\overline{Z}'_{ik} = \frac{j\omega 2^{m-1} \prod_0^m \mu_i}{\pi} \times \int_0^{\infty} \left\{ \frac{e^{-\overline{\alpha}_0 h_2} \prod_1^{m-1} \overline{\alpha}_i \prod_1^m e^{-\overline{\alpha}_i d_i} \left(\overline{DT}_{rec} \right)}{\overline{DTD}_0} \right\} \cos(uy_{ik}) du \tag{10b}$$

where $\overline{DT}_{rec} = \overline{DTD}_m e^{\overline{\alpha}_m (d_m - h_1)} + \overline{DTN}_m e^{-\overline{\alpha}_m (d_m - h_1)}$ and the term products are defined as $\prod_1^m e^{-\overline{\alpha}_i d_i} = e^{-\overline{\alpha}_1 d_1} e^{-\overline{\alpha}_2 d_2} \cdots e^{-\overline{\alpha}_m d_m}$, $\prod_1^{m-1} \overline{\alpha}_i = \overline{\alpha}_1 \cdots \overline{\alpha}_{m-1}$ and $\prod_0^m \mu_i = \mu_0 \mu_1 \mu_2 \cdots \mu_m$. The terms $\overline{DTD}_m$, $\overline{DTN}_m$ and $\overline{DTD}_0$ are calculated recursively by the formulas given in the Appendix (Section 8.1).

The general form of (10b) can be simplified considering that, since most soil types are nonmagnetic, the relative magnetic permeability of all earth layers can be considered to be equal to unity. Furthermore, for frequencies less than 1 MHz, the propagation constants $\overline{\gamma}_i^2 = j\omega\mu_i(\sigma_i + j\omega\varepsilon_i) \approx j\omega\mu_i\sigma_i$, where $i = 0, 1, 2, \ldots, n$. Therefore the $\overline{\alpha}_i$ terms in (10b) can be expressed as $\overline{\alpha}_i = \sqrt{u^2 + j\omega\mu_i\sigma_i}$.

2.3 Determination of per-unit-length self impedance of underground insulated conductor

To determine the per-unit-length self impedance of the underground insulated conductor, the electromagnetic field derived by the underground insulated conductor must be obtained. Thus, assuming a horizontal dipole with moment equal to IdS in the place of the underground insulated conductor i, (11)–(14) become the equations which describe the problem [19]. Considering the origin of the co-ordinate system to be located directly under the insulated conductor i, along the boundary of the regions m and m+1, the following relation is derived. For $\overline{\Pi}_{0x}$:

$$\overline{\Pi}_{0x} = \int_0^{\infty} \overline{f}_0(u) e^{-\overline{\alpha}_0 z} J_0(ru) du, \quad z \geq d_1 + d_2 + \cdots + d_m \tag{11}$$

For $d_2 + \cdots + d_m \leq z \leq d_1 + d_2 + \cdots + d_m$, $\overline{\Pi}_{1x}$ is described by the following equation:

$$\overline{\Pi}_{1x} = \int_0^{\infty} \left[\overline{f}_1(u) e^{-\overline{\alpha}_1 z} + \overline{g}_1(u) e^{\overline{\alpha}_1 z} \right] J_0(ru) du \tag{12}$$

In the mth layer

$$\overline{\Pi}_{mx} = \int_0^{\infty} \left[\overline{f}_{m1}(u) e^{-\overline{\alpha}_m z} + \overline{g}_{m1}(u) e^{\overline{\alpha}_m z} \right] J_0(ru) du, \quad z \geq (d_m - h_1) \tag{13a}$$

and

$$\overline{\Pi}_{mx} = \int_0^{\infty} \left[\overline{f}_{m2}(u) e^{-\overline{\alpha}_m z} + \overline{g}_{m2}(u) e^{\overline{\alpha}_m z} \right] J_0(ru) du, \quad z \leq (d_m - h_1) \tag{13b}$$

Finally $\overline{\Pi}_{nx}$ is given by

$$\overline{\Pi}_{nx} = \int_0^{\infty} \overline{f}_n(u) e^{\overline{\alpha}_n z} J_0(ru) du \tag{14}$$

The $\overline{\Pi}$ functions in (11)–(14) can be determined using the reciprocity theorem [24]. According to this, an equation similar to (10b) can be also obtained if the excitation current is imposed on the underground insulated conductor i, instead of the overhead conductor k. Therefore the per-unit-length mutual impedance $\overline{Z}'_{ik}$ is also given by

$$\overline{Z}'_{ik} = \int_{-\infty}^{\infty} \left[\overline{\gamma}_0^2 \frac{\overline{\Pi}_{0x(z=d_m + d_{m-1} + \cdots + d_2 + d_1 + h_2, y=-y_{ik})}}{IdS} \right] dx \tag{15}$$

Replacing the expression of $\overline{\Pi}_{0x}$ from (11) in (15) and equalising (15) with (10b), $\overline{\Pi}_{0x}$ can be fully determined. Finally, applying the boundary conditions given in [11] at the boundaries of the earth layers, $\overline{\Pi}_{mx}$ can be completely defined. The exact procedure for the determination of the

underground dipole $\overline{\Pi}$ functions is shown in the Appendix (Section 8.2).

The per-unit-length self impedance of the underground insulated conductor i $\overline{Z}'_{ii}$ is then found by integrating $\overline{\Pi}_{mx}$ along the x-axis

$$\overline{Z}'_{ii} = \int_{-\infty}^{\infty} \left[\overline{\gamma}_m^2 \frac{\overline{\Pi}_{mx(z=d_m-h_1, y=r_{ii})}}{IdS} \right] dx \qquad (16)$$

In (16) r_{ii} is the insulation outer radius. The final form of $\overline{Z}'_{ii}$ results as (17)

$$\overline{Z}'_{ii} = \frac{j\omega\mu_m}{2\pi} \int_0^{\infty} \frac{\cos(ur_{ii})}{\overline{\alpha}_m} \times \left\{ e^{-\overline{\alpha}_m d_m} \frac{\begin{array}{c}\left[\overline{DTD}_m e^{\overline{\alpha}_m(d_m-h_1)} + \overline{DTN}_m e^{-\overline{\alpha}_m(d_m-h_1)}\right] \\ \times\left[\overline{TDD}_{m-1} e^{\overline{\alpha}_m h_1} + \overline{TDN}_{m-1} e^{-\overline{\alpha}_m h_1}\right]\end{array}}{\overline{DTD}_0} \right\} du \qquad (17)$$

The terms $\overline{TDD}_{m-1}$, $\overline{TDN}_{m-1}$ are calculated by the recursive formulas given in the Appendix (Section 8.2). In (17) the geometrical configuration and the influence of the earth have been taken into account. Proper internal impedance terms [21, 22] must be added in (17) to account for the skin effect.

3 Remarks on new expressions

A closer examination of the expressions for the per-unit-length mutual and self impedance, as given by (10*b*) and (17), respectively, reveals the following.

Beginning with (10*b*), the $\left[\overline{DTD}_m e^{\overline{\alpha}_m(d_m-h_1)} + \overline{DTN}_m e^{-\overline{\alpha}_m(d_m-h_1)}\right]$ term contains the electromagnetic and geometrical characteristics of the earth layers between the nth and the mth layer, where the insulated conductor i is buried. This term also contains the vertical co-ordinate of the insulated conductor i. The rest of the terms in the numerator of the integral represent the geometrical and electromagnetic characteristics of the air and the earth layers between the first and the mth layer. Finally, the denominator term $\overline{DTD}_0$ includes the electromagnetic and geometrical properties of all the areas between the air and the nth layer.

Assuming that the electromagnetic properties of all earth layers are equal, the existing formula [7] for the calculation of the mutual impedance between overhead and underground insulated conductors for the homogeneous earth case is derived from (10*b*). Furthermore, (10*b*) is also transformed into the well-known Carson formula for the impedances of overhead lines above homogeneous earth.

The expression for the per-unit-length self impedance essentially consists of the following terms.

The first term in the square brackets contains the electromagnetic and geometrical characteristics of the earth layers between the nth and the mth layers. The second term in the square brackets contains the electromagnetic and geometrical characteristics of the areas between the air and the mth layer. The denominator term $\overline{DTD}_0$ includes all the electromagnetic and geometrical properties of the areas between the air and the nth layer. A simplification of (10*b*) and (17) for a two-layer earth case allows a better analysis of the contribution of each individual term involved in the expressions. Assuming the configuration of Fig. 2 and after setting $\overline{\alpha}_0$ equal to u, as in [10], (10*b*) and (17) are simplified

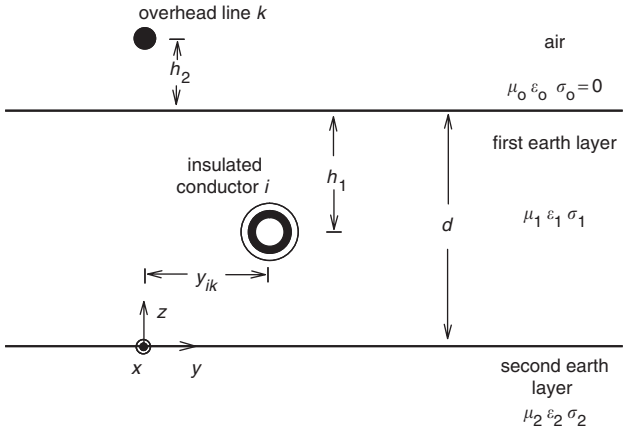

Fig. 2 *Geometric configuration of overhead and underground insulated conductor in two-layer earth*

to (18) and (19), respectively,

$$\overline{Z}'_{ik} = \frac{j\omega\mu_1\mu_0}{\pi} \times \int_0^{\infty} \left[\frac{\begin{array}{l}(\mu_2\overline{\alpha}_1 + \mu_1\overline{\alpha}_2)e^{-\overline{\alpha}_1 h_1} e^{-uh_2} \\ +(\mu_2\overline{\alpha}_1 - \mu_1\overline{\alpha}_2)e^{-\overline{\alpha}_1(2d-h_1)} e^{-uh_2}\end{array}}{(\mu_0\overline{\alpha}_1 + \mu_1 u)(\mu_2\overline{\alpha}_1 + \mu_1\overline{\alpha}_2) + (\mu_2\overline{\alpha}_1 - \mu_1\overline{\alpha}_2)(\mu_1 u - \mu_0\overline{\alpha}_1)e^{-2\overline{\alpha}_1 d}} \right] \cos(uy_{ik})du \qquad (18)$$

$$\overline{Z}'_{ii} = \frac{j\omega\mu_1}{2\pi} \int_0^{\infty} \frac{\cos(ur_{ii})}{\overline{\alpha}_1} \times \left[\frac{\begin{array}{l}\overline{s}_{10}\overline{s}_{21} + \overline{s}_{10}\overline{d}_{21}e^{-2\overline{\alpha}_1(d-h_1)} \\ +\overline{d}_{10}\overline{s}_{21}e^{-2\overline{\alpha}_1 h_1} + \overline{d}_{10}\overline{d}_{21}e^{-2\overline{\alpha}_1 d}\end{array}}{\overline{s}_{10}\overline{s}_{21} - \overline{d}_{10}\overline{d}_{21}e^{-2\overline{\alpha}_1 d}} \right] du \qquad (19)$$

where

$$\overline{s}_{10} = (\mu_0\overline{\alpha}_1 + \mu_1 u),\ \overline{s}_{21} = (\mu_2\overline{\alpha}_1 + \mu_1\overline{\alpha}_2) \text{ and}$$

$$\overline{d}_{21} = (\mu_2\overline{\alpha}_1 - \mu_1\overline{\alpha}_2),\ \overline{d}_{10} = (\mu_0\overline{\alpha}_1 - \mu_1 u)$$

Further observation of (18) reveals that it essentially consists of two terms. The first and dominant one contains two exponential functions that represent the influence of the vertical distance between the underground and the overhead conductor. These exponential functions have as a factor the sum of the electromagnetic properties of the two earth layers. The second term depends on the vertical distance between the overhead conductor and the image of the underground insulated conductor with respect to the two earth layers limit. This term is multiplied with a term corresponding to the difference between the electromagnetic properties of the two earth layers. Thus when the resistivity, permeability and permittivity values of the two earth layers are equal, this term vanishes together with the boundary of the two layers.

On the other hand, observation of (19) shows that it essentially consists of four terms. The first and dominant one contains two terms denoted with the symbol $\overline{s}$ to indicate the sum of the electromagnetic properties of the three different areas: the air, and the first and second earth layers.

The second term depends on the vertical distance between the underground insulated conductor and its image with respect to the limiting surface between the two earth layers. One factor of this term is represented by the symbol $\overline{d}_{21}$ to

indicate the difference between the electromagnetic properties of the two earth layers. Thus when the resistivity, permeability and permittivity values of the two earth layers are equal, this term is set to zero.

The third term refers to the vertical distance between the insulated conductor and its image with respect to the air–earth boundary. One of the factors of the last-mentioned term is $\overline{d}_{10}$, indicating the difference between the electromagnetic properties of the air and the first earth layer.

Finally the fourth term contains an exponential function which depends on the distance between the two images of the insulated conductor with respect to the two boundaries of Fig. 2. As expected, this term has as factors only variables representing differences in the electromagnetic properties of the regions and it vanishes whenever one of the two boundaries diminishes.

4 Numerical integration of impedance formulas

Direct numerical integration is used for the calculation of the semi-infinite integrals in (10*b*) and in (17)–(19). The implementation of a single numerical integration method proved to be inadequate, due to the specific characteristics of the integrals. The presence of the function cos( ) requires the use of a proper numerical method, best suited to follow the oscillations of the integrands. On the other hand, the initial steep descent of the integrands suggests the use of a different numerical integration method in the interval between zero and the first root of the function cos( ). Finally, the exponential functions, which appear in the integrands, lead to the adoption of a method capable of dealing with the effects of such terms.

Following this reasoning, a complex integration scheme is implemented. The 20-point Lobatto rule [25] is applied to the intervals between the subsequent roots of the function cos( ), while the 16-point shifted Gauss–Legendre method [26] is used to calculate the integral between zero and the first root of cos( ). Finally the 35-point shifted Gauss–Laguerre method [26] is also applied, since it is properly fitted for the calculation of semi-infinite integrals with exponential weight functions. A more extensive presentation of the proposed numerical integration scheme can be found in the Appendix (Section 8.3).

This novel integration scheme has been applied successfully to the calculation of the earth return impedances of cables in cases of two-layer and homogeneous earth [19, 20]. In all cases examined the new method proved to be remarkably efficient and numerically stable.

5 Numerical results

The new expressions for the *n*-layered earth model are used to calculate the per-unit-length impedances of the system in Fig. 3. The system consists of a typical single-circuit overhead transmission line with two ground wires. The ground and phase wires are considered to be solid cylindrical conductors with radius 0.004 and 0.0109 m, respectively. The ground wires have a conductivity equal to 3.522×10^6 S/m and a relative permeability equal to 250. The corresponding values for the phase conductors are 3.652×10^7 S/m and 1. The underground insulated metal pipeline has an inner radius equal to 0.195 m and an outer radius of 0.2 m, whereas the insulation thickness is 0.1 m. The conductivity and the relative permeability of the pipe are the same as those of the ground wires. The relative permeability of the insulation, of the air and the relative permittivity of the air are all equal to unity.

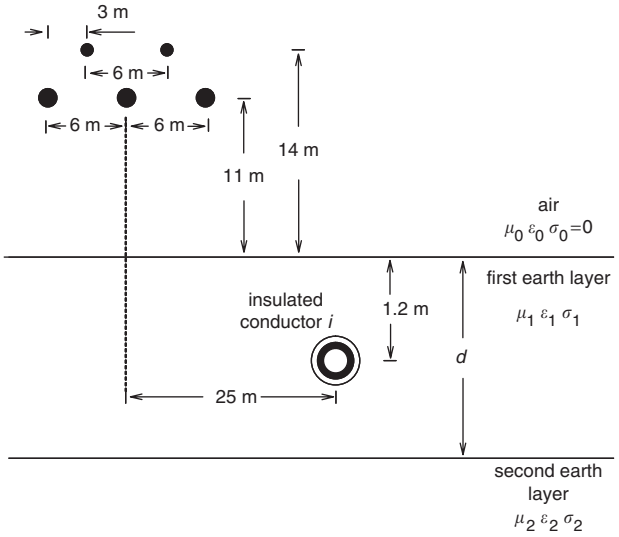

Fig. 3 *Geometric configuration of single-circuit overhead line with two ground wires and underground insulated conductor in two-layer earth*

Table 1: Two-layer earth models

Case	ρ_1 (Ω · m)	ρ_2 (Ω · m)	d (m)
I	372.729	145.259	2.690
II	246.841	1058.79	2.139
III	57.344	96.714	1.651
IV	494.883	93.663	4.370
V	160.776	34.074	1.848
VI	125.526	1093.08	2.713

Six different two-layered earth models, based on actual ground resistivity measurements [12] are investigated. The corresponding data for the resistivities ρ_1 of the first and ρ_2 of the second layer and for the depth d of the first layer are shown in Table 1. The second layer is considered to be of infinite depth.

5.1 Verification of accuracy of new expressions

The complex impedances for the configuration of Fig. 3 are calculated for the six earth models of Table 1 using the proposed formulas of (18) and (19) for the frequency range of 50 Hz to 1 MHz. The novel numerical integration scheme proved to be numerically stable in all cases. The computation time for the numerical integration, with a defined tolerance of 10^{-8}, is less than 15 min for the calculation of a set of 60 impedance matrices using an Intel Pentium IV PC at 2.66 GHz. When the tolerance is defined at 10^{-7}, the computational time is less than 8 min for the same set of the 60 cases.

To check the accuracy of the derived results they are compared with those obtained by a FEM formulation for the same test cases. The FEM package developed at the Power Systems Laboratory of the Aristotle University of Thessaloniki has been used. Introducing a newly developed iteratively adaptive mesh generation technique [27], this package can be applied for the computation of the self and mutual impedances of the conductors of the problem, in unbounded discretisation areas [16].

The relative percent differences between the results by the FEM and the new expressions are calculated using (20), with the results obtained by the FEM used as the reference. These differences for the magnitude of the mutual

impedance between the insulated pipeline and the closest phase wire of the overhead line are shown in Fig. 4. In Fig. 5 the differences between the new expressions and the FEM are presented for the magnitude of the self impedance of the underground insulated conductor.

From these diagrams it is shown that the impedance values calculated using the new expressions show differences less than 0.4% to those by FEM for the frequency range under consideration. The recorded differences for the magnitude and the phase of all impedances of the arrangement are less than 1% justifying the accuracy of the proposed methodology.

$$\text{Relative difference } (\%) = \frac{\left||\overline{Z}_{approach}| - |\overline{Z}_{reference}|\right|}{|\overline{Z}_{reference}|} \times 100 \quad (20)$$

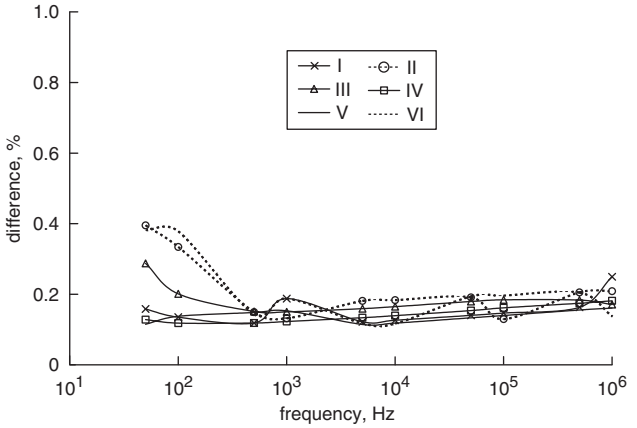

Fig. 4 *Differences in magnitude of mutual impedance between expressions and FEM*

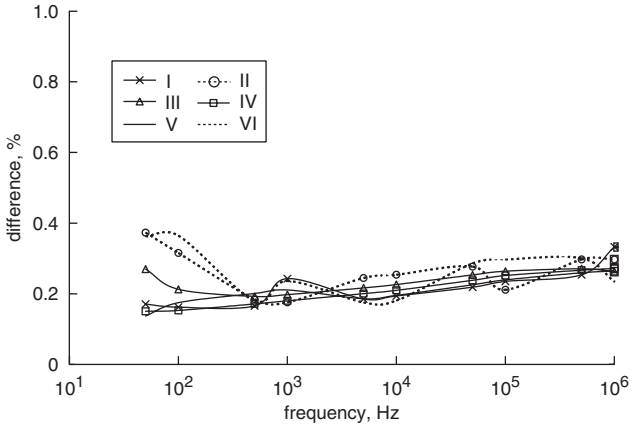

Fig. 5 *Differences in magnitude of self impedance between expressions and FEM*

5.2 Comparison with homogeneous earth case

The scope of the next test is to check the influence of earth stratification on the impedances of the configuration. The complex impedances of the conductors are calculated for the configuration of Fig. 3 and the six earth models of Table 1 using the proposed formulas. The results are compared with the corresponding under the assumption that the earth is homogeneous with a resistivity equal to the resistivity of the first earth layer. The percentage differences calculated using (20) and considering the homogeneous earth case as reference are presented in Fig. 6 for the magnitude of the mutual impedance between the pipeline and the closest phase. They reach up to 80% for high frequencies and for cases of significant divergence between the earth-layer resistivities. Differences up to 30% appear even at power frequency, indicating that earth stratification can affect significantly the system impedances over the whole frequency range.

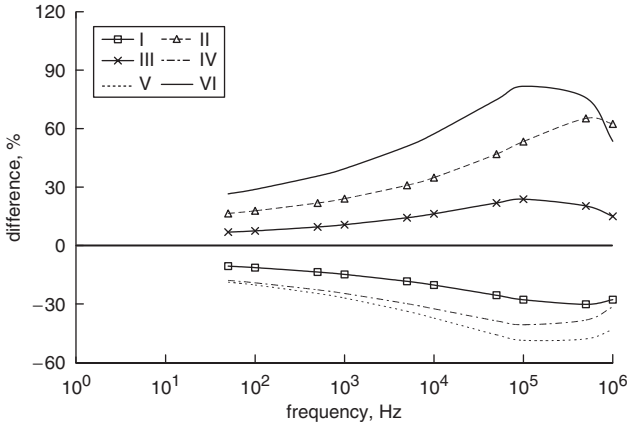

Fig. 6 *Differences in mutual impedance between underground insulated pipeline and overhead line between two-layered and homogeneous earth case*

5.3 Influence of earth stratification on inductive interference between pipeline and overhead line

To investigate the influence of earth stratification on the actual voltages induced on a pipeline, the calculated impedances were implemented in a practical case of inductive interference calculation in the test case of Fig. 3. More specifically, it is assumed that the power line and the pipeline share a common right of way for 25 km, as in [18]. A single-phase to ground fault at phase A is assumed at the end of the right of way, while the other phases remain unloaded. The line supporting towers are located at distances of 250 m and are grounded with 20 Ω resistances. The pipeline has a coating resistance of 20 kΩ m^2 and is insulated at both ends via insulating junctions.

The pipeline is assumed to be buried in each one of the six earth stratification cases of Table 1, while the power line operates at power frequency. Figure 7 shows a typical induced voltage profile along the pipeline, over the value of the fault current, for the case V of Table 1. The dotted line represents the voltage profile for the stratified earth case, while the continuous line corresponds to a homogeneous

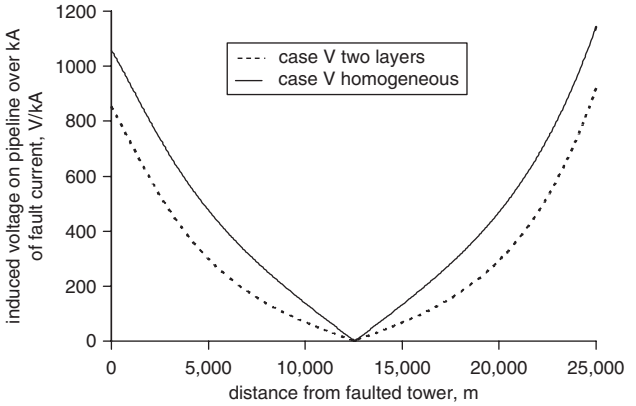

Fig. 7 *Induced voltage along pipeline for case V of Table 1*

earth with a resistivity equal to that of the first layer. It can be seen that earth stratification affects the induced voltage significantly. Table 2 summarises the percent differences between the homogeneous and the two-earth layer case, calculated using (20) with the homogeneous earth results as the reference, for all earth stratification cases of Table 1. The first two columns record the differences at both ends of the pipeline, where the highest induced voltages occur. In the third column the maximum differences, which occur along the pipeline for the length of the common right of way, are presented. The differences are greater than 20% for the higher induced voltages, reaching more than 100% at certain points of the pipeline along the common track.

Finally the influence of earth stratification on the induced voltages is also checked for higher frequencies that may occur during transient conditions. The voltages on the pipeline at the point nearest to the faulted tower are calculated for frequencies from 50 Hz up to 1 MHz and for all cases of Table 1. The absolute percentage differences between the voltages for homogeneous and the two-earth layer case are summarised in Fig. 8. It can be seen that the recorded differences more or less follow the corresponding of the mutual impedances in Fig. 6, as the induced voltages depend mainly on the mutual coupling, which is in turn most significantly affected by the earth return path.

All these results show that it is important to include earth stratification in the electromagnetic interference calculations and this can be efficiently accomplished using the proposed formulation.

Table 2: Percentage differences between induced voltages for homogeneous and two-layer earth cases at 50 Hz

Case	Pipeline end near fault, %	Pipeline end near source, %	Maximum difference, %
I	14.32	14.09	94.45
II	7.13	7.71	71.05
III	0.24	0.74	71.48
IV	22.28	22.21	103.77
V	24.24	24.14	102.41
VI	12.90	13.56	62.07

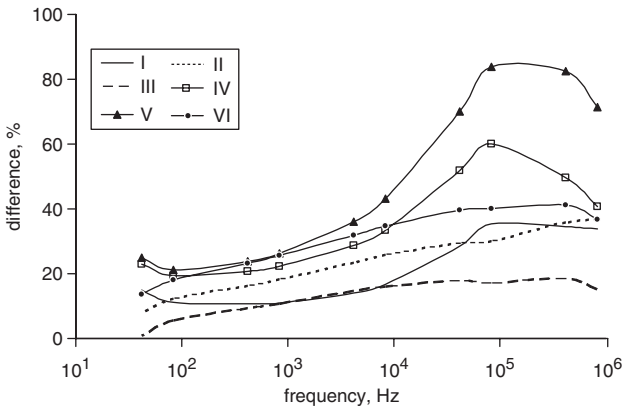

Fig. 8 *Absolute percent differences in induced voltage on pipeline between homogeneous and two-earth layer case*

6 Conclusions

The problem of the calculation of the complex impedances of a system comprising of overhead and underground insulated conductors in a multilayered earth has been addressed. Analytic expressions for the self impedance of the underground insulated conductor and the mutual impedances between the underground and the overhead conductors are derived by a solution of the electromagnetic field equations. For the numerical evaluation of the semi-infinite integrals involved in the derived expressions, a new numerical integration scheme, based on proper combinations of three integration methods, is used. The proposed formulation is applied for the computation of the electrical parameters needed for an interference computation between a typical single circuit overhead transmission line and an underground insulated metal pipeline, buried in the first layer of a variable two-layer earth structure.

To check the accuracy of the results obtained by the new analytic expressions, they are compared with the corresponding obtained by a suitable FEM formulation. The recorded differences in the self and mutual impedance magnitudes and arguments are less than 1% over a wide frequency range from power frequency up to 1 MHz, covering all possible transmission line operational states. The integration scheme proved to be numerically stable and efficient in all examined cases.

The impedances calculated by the expressions for a two-layer earth, show significant differences compared to those for the homogeneous earth, even at power frequency, reaching up to 80% for the cases of great divergence between the layer resistivities and for high frequencies.

The calculated impedances are used in a practical electromagnetic interference calculation. Results for the induced voltage along a pipeline, sharing a common right of way of 25 km with an overhead power line, showed that it may differ up to 25% in its maximum value, due to the earth stratification, even at power frequency. This difference is further amplified for higher frequencies, showing that earth stratification cannot be disregarded. The proposed formulation, together with the new numerical integration method, offers an efficient tool for the electromagnetic interference computations. The use of the proposed methodology eliminates the need for complex modelling in the estimation of the system parameters and avoids approximations, which may lead to inaccurate results.

7 References

1 Dabkowski, J., and Taflove, A.: 'A mutual design consideration for overhead AC transmission lines and gas pipelines' (EPRI Report EL-904, 1978, Vol. 1)
2 Frazier, M.J.: 'Power-line induced AC potential on natural gas pipelines for complex rights-of-way configurations' (EPRI Report EL-3106, AGA L51418, 1984)
3 Dawalibi, F.P., Southey, R.D., Malric, Y., and Tavcar, W.: 'Power-line fault current coupling to nearby natural gas pipelines' (EPRI Report EL 5472, AGA, L51537, 1987, s1 & 2)
4 CIGRE Guide: 'Concerning influence of high voltage AC power systems on metallic pipelines'. CIGRE Working group 36.02, 1995
5 Haubrich, H.J., Flechner, B.A., and Machczyński, W.: 'A universal model for the computation of the electromagnetic interference on earth return circuits', *IEEE Trans. Power Deliv.*, 1994, **PWRD-9**, (3), pp. 1593–1599
6 Carson, J.R.: 'Wave propagation in overhead wires with ground return', *Bell Syst. Tech. J.*, 1926, **5**, pp. 539–554
7 Pollaczek, F.: 'Ueber das Feld einer unendlich langen wechselstromdurchflossenen Einfachleitung', *Elektr. Nachr.*, 1926, **3**, (4), pp. 339–359
8 CCITT: 'Directives concerning the protection of telecommunication lines against harmful effects from electric power and electrified railway lines, Vol. 3, Capacitive, inductive and conductive coupling: Physical theory and calculation methods' (ITU, Geneva, 1989)
9 Uribe, F.A.: 'Mutual ground impedance between overhead and underground transmission cables' Paper IPST05-151, presented at the Int. Conf. on Power System Transients, 2005, available through www.ipst.org
10 Sunde, E.D.: 'Earth conduction effects in transmission systems' (Dover Publications, 1968, 2nd edn), pp. 99–139

11 Nakagawa, M., Ametani, A., and Iwamoto, K.: 'Further studies on wave propagation in overhead transmission lines with earth return: impedance of stratified earth', *Proc. IEE*, 1973, **120**, (12), pp. 1521–1528
12 Alamo, J.L.: 'A comparison among different techniques to achieve an optimum estimation of electrical grounding parameters in two-layered earth', *IEEE Trans. Power Deliv.*, 1993, **PWRD-8**, (4), pp. 1890–1899
13 Gonos, I.F., and Stathopoulos, I.A.: 'Estimation of multilayer soil parameters using genetic algorithms', *IEEE Trans. Power Deliv.*, 2005, **PWRD-20**, (1), pp. 100–106
14 Zhang, B., Cui, X., Li, L., and He, J.: 'Parameter estimation of horizontal multilayer earth by complex image method', *IEEE Trans. Power Deliv.*, 2005, **PWRD-20**, (2), pp. 1394–1401
15 Lagace, P.J., Fortin, J., and Crainic, E.D.: 'Interpretation of resistivity sounding measurements in *N*-layer soil using electrostatic image', *IEEE Trans. Power Deliv.*, 1996, **PWRD-11**, (3), pp. 1349–1354
16 Papagiannis, G.K., Triantafyllidis, D.G., and Labridis, D.P.: 'A one-step finite-element formulation for the modelling of single and double-circuit transmission lines', *IEEE Trans. Power Syst.*, 2000, **15**, (1), pp. 33–38
17 Christoforidis, G.C., Labridis, D.P., and Dokopoulos, P.S.: 'A hybrid method for calculating the inductive interference caused by faulted power lines to nearby pipelines', *IEEE Trans. Power Deliv.*, 2005, **PWRD-20**, (2), pp. 1465–1473
18 Christoforidis, G.C., Labridis, D.P., and Dokopoulos, P.S.: 'Inductive interference on pipelines buried in multilayer soil, due to magnetic fields from nearby faulted power lines', *IEEE Trans. Electromagn. Compat.*, 2005, **47**, (2), pp. 254–262
19 Tsiamitros, D.A., Papagiannis, G.K., Labridis, D.P., and Dokopoulos, P.S.: 'Earth return path impedances of underground cables for the two-layer earth case', *IEEE Trans. Power Deliv.*, 2005, **PWRD-20**, (3), pp. 2174–2181
20 Papagiannis, G.K., Tsiamitros, D.A., Labridis, D.P., and Dokopoulos, P.S.: 'Direct numerical evaluation of the earth return path impedances of underground cables', *IEE Proc., Gener., Transm. Distrib.*, 2005, **152**, (3), pp. 321–328
21 Dommel, H.W.: 'Electromagnetic transients program reference manual' (Bonneville Power Administration, OR, Portland, 1986), pp. 5-15–5-22
22 Ametani, A.: 'A general formulation of impedance and admittance of cables', *IEEE Trans. Power Appar. Syst.*, 1980, **PAS-99**, (3), pp. 902–910
23 Abramowitz, M., and Stegun, I.: 'Handbook of mathematical functions' (Dover Publications, 1972), pp. 479–494
24 Dorf, R.C.: 'The electrical engineering handbook' (CRC Press, 1993), pp. 77–79
25 Davies, P., and Rabinowitch, P.: 'Methods of numerical integration' (Academic Press, 2nd Edn. 1984), pp. 104, 223
26 Ralston, A., and Rabinowitch, P.: 'A first course in numerical analysis' (McGraw-Hill, 2nd edn., 1988), pp. 100, 106
27 Labridis, D.P.: 'Comparative presentation of criteria used for adaptive finite-element mesh generation in multiconductor eddy current problems', *IEEE Trans. Magn.*, 2000, **36**, (1), pp. 267–280

8 Appendix

8.1 Field derived by overhead dipole

Substituting the exact expressions of $\overline{\Pi}'_{(k-1)x}$ and $\overline{\Pi}'_{kx}$ in (5) and (6), the following general equations are derived:

$$\overline{\gamma}_{k-1}^2\left(\overline{f}'_{k-1}e^{\overline{\alpha}_{k-1}(d_k+d_{k+1}+\cdots+d_m)}+\overline{g}'_{k-1}e^{-\overline{\alpha}_{k-1}(d_k+d_{k+1}+\cdots+d_m)}\right)=\overline{\gamma}_k^2\left(\overline{f}'_k e^{\overline{\alpha}_k(d_k+d_{k+1}+\cdots+d_m)}+\overline{g}'_k e^{-\overline{\alpha}_k(d_k+d_{k+1}+\cdots+d_m)}\right) \tag{21}$$

$$\frac{\overline{\alpha}_{k-1}}{\mu_{k-1}}\overline{\gamma}_{k-1}^2\left(\overline{f}'_{k-1}e^{\overline{\alpha}_{k-1}(d_k+d_{k+1}+\cdots+d_m)}-\overline{g}'_{k-1}e^{-\overline{\alpha}_{k-1}(d_k+d_{k+1}+\cdots+d_m)}\right)=\frac{\overline{\alpha}_k}{\mu_k}\overline{\gamma}_k^2\left(\overline{f}'_k e^{\overline{\alpha}_k(d_k+d_{k+1}+\cdots+d_m)}-\overline{g}'_k e^{-\overline{\alpha}_k(d_k+d_{k+1}+\cdots+d_m)}\right) \tag{22}$$

Starting from the last two earth layers, for $k=n$, (21) and (22) are transformed into

$$\overline{\gamma}_{n-1}^2\left(\overline{f}'_{n-1}e^{\overline{\alpha}_{n-1}[-(d_{n-1}+d_{n-2}+\cdots+d_{m+1})]}+\overline{g}'_{n-1}e^{-\overline{\alpha}_{n-1}[-(d_{n-1}+d_{n-2}+\cdots+d_{m+1})]}\right)=\overline{\gamma}_n^2\left(\overline{f}'_n e^{\overline{\alpha}_n[-(d_{n-1}+d_{n-2}+\cdots+d_{m+1})]}\right) \tag{23}$$

$$\frac{\overline{\alpha}_{n-1}}{\mu_{n-1}}\overline{\gamma}_{n-1}^2\left(\overline{f}'_{n-1}e^{\overline{\alpha}_{n-1}[-(d_{n-1}+d_{n-2}+\cdots+d_{m+1})]}-\overline{g}'_{n-1}e^{-\overline{\alpha}_{n-1}[-(d_{n-1}+d_{n-2}+\cdots+d_{m+1})]}\right)=\frac{\overline{\alpha}_n}{\mu_n}\overline{\gamma}_n^2\left(\overline{f}'_n e^{\overline{\alpha}_n[-(d_{n-1}+d_{n-2}+\cdots+d_{m+1})]}\right) \tag{24}$$

After multiplying (23) with the factor $\overline{\alpha}_n/\mu_n$, the right-hand parts of (23) and (24) become equal. Equalising the left-hand parts of the two equations the following relation between $\overline{f}'_{n-1}$ and $\overline{g}'_{n-1}$ is obtained:

$$\overline{g}'_{n-1}(u)=\overline{f}'_{n-1}(u)\frac{(\mu_n\overline{\alpha}_{n-1}-\mu_{n-1}\overline{\alpha}_n)}{(\mu_n\overline{\alpha}_{n-1}+\mu_{n-1}\overline{\alpha}_n)}e^{2\overline{\alpha}_{n-1}[-(d_{n-1}+d_{n-2}+\cdots+d_{m+1})]} \tag{25}$$

For $k=n-1$, (21) and (22) are transformed into

$$\begin{aligned}&\overline{\gamma}_{n-2}^2\left(\overline{f}'_{n-2}e^{\overline{\alpha}_{n-2}[-(d_{n-2}+d_{n-3}+\cdots+d_{m+1})]}+\overline{g}'_{n-2}e^{-\overline{\alpha}_{n-2}[-(d_{n-2}+d_{n-3}+\cdots+d_{m+1})]}\right)\\&=\overline{\gamma}_{n-1}^2\left(\overline{f}'_{n-1}e^{-\overline{\alpha}_{n-1}[-(d_{n-1}+d_{n-2}+\cdots+d_{m+1})]}\right)+\overline{g}'_{n-1}e^{\overline{\alpha}_{n-1}[-(d_{n-2}+d_{n-3}+\cdots+d_{m+1})]}\Big)\end{aligned} \tag{26}$$

$$\begin{aligned}&\frac{\overline{\alpha}_{n-2}}{\mu_{n-2}}\overline{\gamma}_{n-2}^2\left(\overline{f}'_{n-2}e^{\overline{\alpha}_{n-2}[-(d_{n-2}+d_{n-3}+\cdots+d_{m+1})]}-\overline{g}'_{n-2}e^{-\overline{\alpha}_{n-2}[-(d_{n-2}+d_{n-3}+\cdots+d_{m+1})]}\right)\\&=\frac{\overline{\alpha}_{n-1}}{\mu_{n-1}}\overline{\gamma}_{n-1}^2\left(\overline{f}'_{n-1}e^{\overline{\alpha}_{n-1}[-(d_{n-2}+d_{n-3}+\cdots+d_{m+1})]}-\overline{g}'_{n-1}e^{-\overline{\alpha}_{n-1}[-(d_{n-2}+d_{n-3}+\cdots+d_{m+1})]}\right)\end{aligned} \tag{27}$$

Substituting $\overline{g}'_{n-1}$ from (25), in (26) and (27) and eliminating $\overline{f}'_{n-1}$ from the latter equations, a new equation is derived, containing only the functions $\overline{g}'_{n-2}$ and $\overline{f}'_{n-2}$.

In a similar way the following general equation results:

$$\overline{g}'_i(u)=\overline{f}'_i(u)\frac{\overline{DTN}_i}{\overline{DTD}_i}e^{2\overline{\alpha}_i ZL_i} \tag{28}$$

where $i=1,2,\ldots,n$, ZL_i is the z-co-ordinate of the ith layer lower boundary and

$$\begin{aligned}\overline{DTN}_i=&(\mu_{i+1}\overline{\alpha}_i-\mu_i\overline{\alpha}_{i+1})\overline{DTD}_{i+1}\\&+(\mu_{i+1}\overline{\alpha}_i+\mu_i\overline{\alpha}_{i+1})\overline{DTN}_{i+1}e^{-2\overline{\alpha}_{i+1}d_{i+1}}\end{aligned} \tag{29}$$

$$\begin{aligned}\overline{DTD}_i=&(\mu_{i+1}\overline{\alpha}_i+\mu_i\overline{\alpha}_{i+1})\overline{DTD}_{i+1}\\&+(\mu_{i+1}\overline{\alpha}_i-\mu_i\overline{\alpha}_{i+1})\overline{DTN}_{i+1}e^{-2\overline{\alpha}_{i+1}d_{i+1}}\end{aligned} \tag{30}$$

$$\overline{DTN}_n=0 \tag{31}$$

$$\overline{DTD}_n=1 \tag{32}$$

Substituting (28) in (7) and (8) and eliminating $\overline{f}'_1(u)$ from (7) and (8), $\overline{g}'_0(u)$ is obtained

$$\overline{g}'_0(u)=\overline{C}\frac{u}{\overline{\alpha}_0}e^{-\overline{\alpha}_0 h_2}e^{\overline{\alpha}_0(d_1+d_2+\cdots+d_m)}\frac{\overline{DTN}_0}{\overline{DTD}_0} \tag{33}$$

Replacing $\overline{g}_0'(u)$ from (33) and $\overline{g}_1'(u)$ from (28) in (7), $\overline{f}_1'(u)$ is obtained

$$\overline{f}_1'(u) = \overline{C}\frac{u}{\overline{\alpha}_0}e^{-\overline{\alpha}_0 h_2}\frac{\overline{\gamma}_0^2}{\overline{\gamma}_1^2}\frac{2\mu_1\overline{\alpha}_0\overline{DTD}_1}{\overline{DTD}_0}e^{-\overline{\alpha}_1(d_1+d_2+\cdots+d_m)} \quad (34)$$

Finally the following general equation is derived for $\overline{f}_1'(u)$:

$$\overline{f}_i'(u) = \overline{C}\frac{u}{\overline{\alpha}_0}e^{-\overline{\alpha}_0 h_2}\frac{\overline{\gamma}_0^2}{\overline{\gamma}_i^2} \times \frac{2^i\left(\prod_1^i \mu_j\right)\left(\prod_0^{i-1}\overline{\alpha}_j\right)\left(\prod_1^{i-1}e^{-\overline{\alpha}_j d_j}\right)\overline{DTD}_i}{\overline{DTD}_0}e^{-\overline{\alpha}_i ZH_i} \quad (35)$$

where ZH_i is the z-co-ordinate of the ith layer upper boundary.

8.2 Field derived by underground dipole

Replacing the expression of $\overline{\Pi}_{0x}$ from (11) in (15), the per-unit-length mutual impedance $\overline{Z}_{ik}'$ between the insulated conductor i and the overhead conductor k is

$$\overline{Z}_{ik}' = \overline{\gamma}_0^2\int_0^\infty \frac{2\overline{f}_0(u)e^{-\overline{\alpha}_0(d_m+\cdots+d_2+d_1+h_2)}}{IdS}\frac{\cos(uy_{ik})}{u}du \quad (36)$$

Equalising (36) with (10b), the resulting expression for $\overline{f}_0(u)$ is derived and shown in (37), where $\overline{C}_m = \frac{j\omega\mu_m IdS}{4\pi\overline{\gamma}_m^2}$

$$\begin{aligned}\overline{f}_0(u) &= 2^m\overline{C}_m\frac{u}{\overline{\alpha}_0}\frac{\overline{\gamma}_m^2}{\overline{\gamma}_0^2}\frac{\left(\prod_0^{m-1}\mu_i\right)\left(\prod_0^{m-1}\overline{\alpha}_i\right)\left(\prod_0^{m-1}e^{-\overline{\alpha}_i d_i}\right)}{\overline{DTD}_0} \\ &\quad\times\left[\overline{DTD}_m e^{\overline{\alpha}_m(d_m-h_1)} + \overline{DTN}_m e^{-\overline{\alpha}_m(d_m-h_1)}\right]e^{\overline{\alpha}_0(d_1+d_2+\cdots+d_m)} \\ &= 2^m\overline{C}_m u\frac{\overline{\gamma}_m^2}{\overline{\gamma}_0^2}\mu_0\overline{K}_1(u)e^{\overline{\alpha}_0(d_1+d_2+\cdots+d_m)}\end{aligned} \quad (37)$$

Applying the boundary conditions (5) and (6) for the system of (11)–(13a), 2m equations like the following are derived:

$$\begin{aligned}&\overline{\gamma}_0^2\left(2^m\overline{C}_m u\frac{\overline{\gamma}_m^2}{\overline{\gamma}_0^2}\mu_0\overline{\mathrm{K}}_1(u)\right) \\ &\quad= \overline{\gamma}_1^2\left(\overline{f}_1(u)e^{-\overline{\alpha}_1(d_m+\cdots+d_2+d_1)} + \overline{g}_1(u)e^{\overline{\alpha}_1(d_m+\cdots+d_2+d_1)}\right)\end{aligned} \quad (38)$$

$$\begin{aligned}&-\frac{\overline{\alpha}_0}{\mu_0}\overline{\gamma}_0^2\left(2^m\overline{C}_m u\frac{\overline{\gamma}_m^2}{\overline{\gamma}_0^2}\mu_0\overline{\mathrm{K}}_1(u)\right) \\ &\quad= \frac{\overline{\alpha}_1}{\mu_1}\overline{\gamma}_1^2\left(-\overline{f}_1(u)e^{-\overline{\alpha}_1(d_m+\cdots+d_2+d_1)} + \overline{g}_1(u)e^{\overline{\alpha}_1(d_m+\cdots+d_2+d_1)}\right)\end{aligned} \quad (39)$$

$$\begin{aligned}&\overline{\gamma}_1^2\left(\overline{f}_1(u)e^{-\overline{\alpha}_1(d_m+\cdots+d_3+d_2)} + \overline{g}_1(u)e^{\overline{\alpha}_1(d_m+\cdots+d_3+d_2)}\right) \\ &\quad= \overline{\gamma}_2^2\left(\overline{f}_2(u)e^{-\overline{\alpha}_2(d_m+\cdots+d_3+d_2)} + \overline{g}_2(u)e^{\overline{\alpha}_2(d_m+\cdots+d_3+d_2)}\right)\end{aligned} \quad (40)$$

$$\begin{aligned}&\frac{\overline{\alpha}_1}{\mu_1}\overline{\gamma}_1^2\left(-\overline{f}_1(u)e^{-\overline{\alpha}_1(d_m+\cdots+d_3+d_2)} + \overline{g}_1(u)e^{\overline{\alpha}_1(d_m+\cdots+d_3+d_2)}\right) \\ &\quad= \frac{\overline{\alpha}_2}{\mu_2}\overline{\gamma}_2^2\left(-\overline{f}_2(u)e^{-\overline{\alpha}_2(d_m+\cdots+d_3+d_2)} + \overline{g}_2(u)e^{\overline{\alpha}_2(d_m+\cdots+d_3+d_2)}\right)\end{aligned} \quad (41)$$

From the system of 2m equations, applying a similar procedure as in Section 8.1, $\overline{f}_l(u)$, $\overline{g}_l(u)$ are derived, where $l = 0, 1, 2, \ldots, m$

$$\overline{g}_l(u) = \overline{f}_l(u)\frac{\overline{TDN}_{l-1}}{\overline{TDD}_{l-1}}e^{-2\overline{\alpha}_l(d_m+d_{m-1}+\cdots+d_l)} \quad (42)$$

$$\begin{aligned}\overline{f}_l(u) &= \frac{2^{m-l}\overline{C}_m u\mu_0\left(\prod_1^{l-1}e^{\overline{\alpha}_i d_i}\right)}{\left(\prod_0^{l-1}\mu_i\right)\left(\prod_1^{l}\overline{\alpha}_i\right)}\frac{\overline{\gamma}_m^2}{\overline{\gamma}_l^2} \\ &\quad\cdot\overline{K}_1(u)\overline{TDD}_{l-1}e^{\overline{\alpha}_l(d_m+d_{m-1}+\cdots+d_l)}\end{aligned} \quad (43)$$

In (42) and (43)

$$\overline{TDD}_{-1} = 1 \quad (44)$$

$$\overline{TDN}_{-1} = 0 \quad (45)$$

$$\begin{aligned}\overline{TDD}_{l-1} &= (\mu_{l-1}\overline{\alpha}_l + \mu_l\overline{\alpha}_{l-1})\overline{TDD}_{l-2} \\ &\quad+ (\mu_{l-1}\overline{\alpha}_l - \mu_l\overline{\alpha}_{l-1})\overline{TDN}_{l-2}e^{-2\overline{\alpha}_{l-1}d_{l-1}}\end{aligned} \quad (46)$$

$$\begin{aligned}\overline{TDN}_{l-1} &= (\mu_{l-1}\overline{\alpha}_l - \mu_l\overline{\alpha}_{l-1})\overline{TDD}_{l-2} \\ &\quad+ (\mu_{l-1}\overline{\alpha}_l + \mu_l\overline{\alpha}_{l-1})\overline{TDN}_{l-2}e^{-2\overline{\alpha}_{l-1}d_{l-1}}\end{aligned} \quad (47)$$

When l=m the functions $\overline{f}_l(u)$ and $\overline{g}_l(u)$ are transformed into $\overline{f}_{m1}(u)$ and $\overline{g}_{m1}(u)$. Thus $\overline{\Pi}_{mx}$ in (13a) is completely defined.

8.3 Numerical integration technique

For the calculation of (10b) and (17)–(19), three numerical integration methods are implemented as follows.

When the cos( ) terms are not equal to one, the interval between zero and the first root of $\cos(uy_{ik})$ or $\cos(ur_{ii})$ is divided into the following subintervals:

$$\left(0, \frac{\pi 10^{-6}}{2y}\right), \left(\frac{\pi 10^{-6}}{2y}, \frac{\pi 10^{-5}}{2y}\right), \left(\frac{\pi 10^{-5}}{2y}, \frac{\pi 10^{-4}}{2y}\right)\ldots, \left(\frac{0.1\pi}{2y}, \frac{\pi}{2y}\right)$$

where y is y_{ik} or r_{ii}. In each of these subintervals the complex integrals are calculated using the shifted 16-point Gauss–Legendre method [26]. Then, in the intervals between the subsequent roots of $\cos(uy)$, the 20-point Lobatto rule [25] is used. The procedure stops when the absolute value of the calculated integral between two subsequent roots is less than a user predefined tolerance for both the real and the imaginary part of the integral.

If the horizontal distance y_{ik} is zero, the integration procedure is different. The shifted 16-point Gauss–Legendre method is again applied in the same way between zero and $u_o = 2\pi$. Then the shifted 35-point Gauss–Laguerre method [25] is used for the evaluation of the rest of the integral, after the integrand is scaled by the term $e^{|h_1-h_2|u}$. The procedure is repeated iteratively. In each iteration the use of the Gauss–Legendre method is extended by $2u_o$ intervals to the right of u_o, while the Gauss–Laguerre method is implemented for the calculation of the rest integral until infinity. Convergence is achieved when the absolute difference between two succedent values of the calculated integral is less than a user predefined tolerance.